MULTICRYSTALLINE SiGe SOLAR CELLS WITH Ge CONTENT ABOVE 10 AT%

P. Geiger, P. Raue[1], G. Hahn, P. Fath, E. Bucher, E. Buhrig[2], H.J. Möller[1]

Universität Konstanz, Fachbereich Physik, Fach X916, 78457 Konstanz, Germany
Tel.: +49-7531-88-2132, Fax: +49-7531-88-3895, e-mail patric.geiger@uni-konstanz.de
[1]Institute of Experimental Physics, TU Bergakademie Freiberg, D-09596 Freiberg, Germany
[2]Institute of Nonferrus Metals, TU Bergakademie Freiberg, D-09596 Freiberg, Germany

ABSTRACT: In the present study we investigate the manufacturing of multicrystalline (mc) solar cells with a low germanium content using a modified Si solar cell process. For this purpose mc $Si_{1-x}Ge_x$ ingots were grown in an induction heated furnace using the Bridgman technique. In this way ingots with a diameter of about 3.7 cm and a length of 4.5 cm have been obtained. The Ge concentration in the investigated samples is above 10 at%.
In order to study the material properties of the obtained alloys etch pit density and resistance measurements have been performed on the SiGe wafers. Temperature dependent Hall measurements reveal acoustic phonon scattering to be the dominating scattering mechanism at room temperature while the acceptor activation energy level of boron in SiGe seems to be slightly lower than in crystalline Si. With a not yet optimized solar cell process an efficiency of 4.8% (wafer area 2.8 cm^2, reflectivity > 40% at 905 nm) has been achieved. In contradiction to theoretical considerations the IQE in the long wavelength range does not exceed the one of similarly processed Si wafers. This might be caused by too small diffusion lengths within the SiGe samples.
Keywords: Silicon-Germanium – 1: Multi-Crystalline – 2: Manufacturing and Processing – 3

1. INTRODUCTION

SiGe crystals can be of interest for the production of solar cells, especially in conjunction with tandem solar cell concepts. Cells made out of this material should in principle offer higher values of the Internal Quantum Efficiency (IQE) in the long wavelength range as compared to pure crystalline Si. The reason for this behaviour is the more narrow bandgap of the alloyed crystal. As the SiGe system is completely miscible the bandgap as well as other physical properties can be altered by simply changing the composition of the alloy. The growth of large single crystals, especially with Ge concentrations in the range of 30 - 70 at%, is difficult. As multicrystalline (mc) ingots can be grown more easily, it might be a promising way to use mc SiGe wafers for the manufacturing of solar cells instead of monocrystalline ones.

2. CRYSTAL GROWTH

The multicrystalline $Si_{1-x}Ge_x$ ingots investigated in the present study have been grown in an induction heated furnace (10 kHz) using the Bridgman technique. A graphite mold supported the quartz crucible in which the alloy crystallized. In order to avoid sticking and cracking of the ingot during cooling down, the walls of the crucible were coated with a Si_3N_4 layer. In this way ingots with a diameter of about 3.7 cm and a length of 4.5 cm have been obtained.

Polycrystalline SiGe crystals with a Ge content of up to 23 at% and fluctuations of this content like the one given in Fig. 1 could have been grown so far [1]. The wafers for the solar cells presented in this study were cut horizontal to the solidification front from the upper part of the crystal and show a Ge content of 11 at%. The remaining SiGe crystal was cut into further vertical and horizontal wafers. All wafers were polished with diamond paste.

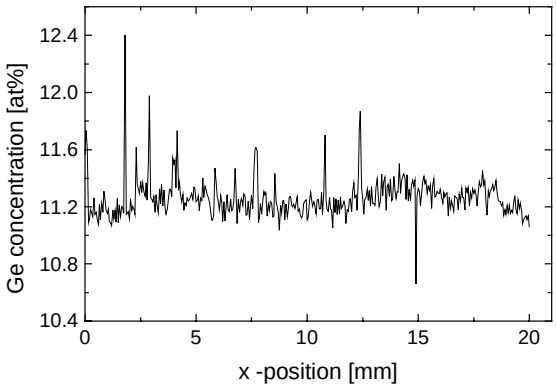

Figure 1: Germanium concentration measured on a vertical cut of the crystal at the height of wafer SiGe#1 using back-scattered electrons in a microprobe.

A two minute treatment with Secco-etchant [2] was found to be a good preparation of the samples for detecting dislocations and grain boundaries. For this purpose etch pit density (EPD) measurements have been performed using a light microscope combined with a computer assisted image processing system. The data has been checked and corrected manually. For a wafer close to those used for solar cell processing, i.e. SiGe#1 and #2, an EPD of $2.5 \cdot 10^5$ cm^{-2} has been found. Twinned regions like the one shown in Fig. 2 are typical crystal defects of the investigated SiGe polycrystals.

The crystal has been doped with boron. Due to segregation during growth the resistance increases from 600 mΩcm close to the bottom part of the crystal up to 800 mΩcm in the upper part. Fig. 3 shows that the resistivity is more homogeneous in the upper than in the lower part of the crystal.

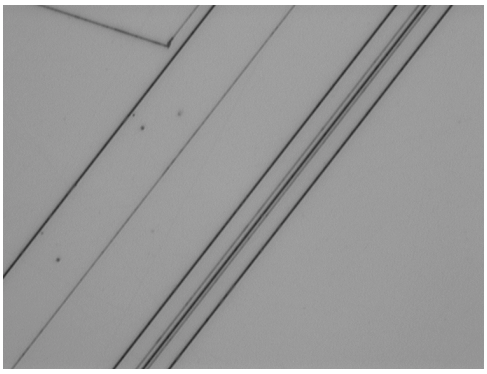

Figure 2: A wafer once located close to SiGe#1 and #2 after two minutes of Secco-etching showing a twinned region (image size 150 x 115 µm^2). The etch-pit-density is $2.5 \cdot 10^5$ cm^{-2}.

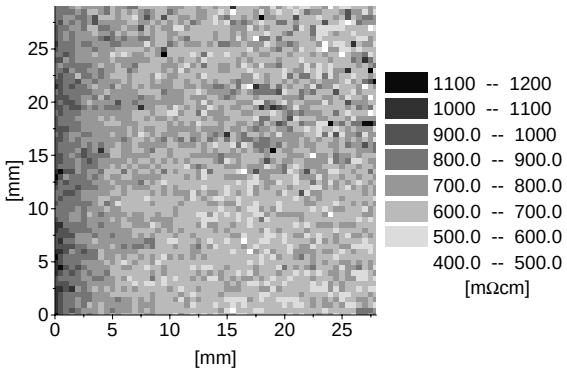

Figure 3: Resistance topogram of a vertical cut of the grown crystal. The left edge corresponds to the top of the crystal, the right to the bottom.

3. ELECTRICAL TRANSPORT PROPERTIES

After defect etching and contact formation [3] temperature dependent Hall measurements have been performed in order to study the electrical transport properties of the SiGe material. Fig. 4 shows the obtained Hall mobilities $\mu_H(T)$ of two different multicrystalline SiGe samples originating from the same wafers as the solar cells discussed in the following sections. Information about the scattering mechanisms of the majority charge carriers can be obtained by fitting these curves in the high temperature range [4]. In case of the investigated samples this procedure leeds to a $T^{-1.5}$ dependence of the mobilities. The same value is theoretically predicted for charge carrier scattering at acoustic phonons in non degenerated semiconductors [4].

It is possible to reveal the temperature dependent majority charge carrier densities $p(T)$ from the same measurements. Those of the investigated SiGe samples given in Fig. 5 show an exponential thermal activation behaviour for temperatures lower than 200 K. As temperature increases electrons of the valence band occupy the boron acceptor levels and the hole concentration, i.e. p, increases. By fitting the data the acceptor activation energy ΔE_A can be derived. The resulting activation energies are given in Fig. 5. According to these values boron seems to be a slightly less deep acceptor in multicrystalline SiGe than in p-type Si for which a ΔE_A of about 45 meV is given in literature [5].

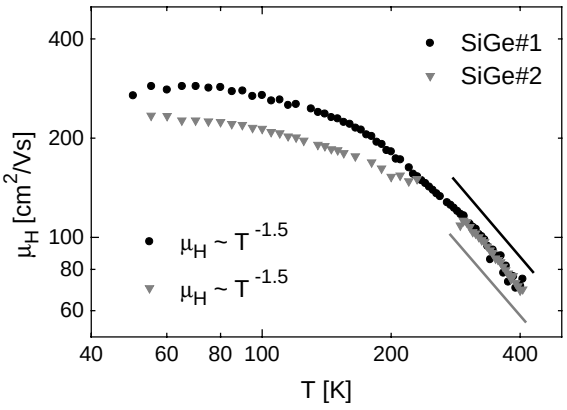

Figure 4: Hall mobility $\mu_H(T)$ of different multicrystalline SiGe samples and corresponding temperature exponents obtained by fitting the curves in the high temperature range.

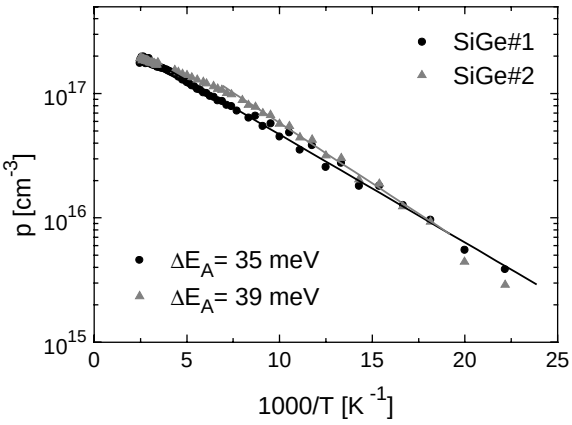

Figure 5: Majority charge carrier density $p(T)$ and corresponding acceptor activation energies.

4. SOLAR CELL PROCESSING

For the manufacturing of SiGe solar cells we used a slightly modified standard Si solar cell process. The wafers were first defect etched in order to remove the surface damage. Afterwards they underwent a cleaning procedure described in [6]. In the next step a phosphorus containing paste was printed onto the wafers using a conventional screen printer. The following diffusion was performed in a commercial belt furnace. The screen printer as well as the belt furnace are normally used for the printing and firing of metal contacts and phosphorus doped emitters in a pilot line of low cost silicon solar cells. In this way we obtained a sheet resistance of 28 – 30 Ω/sq on simultaneously processed monocrystalline Cz-Si test wafers.

As it is known from multicrystalline silicon materials that Al-gettering is an adequate way of enhancing the diffusion length L_{Diff}, such a step was also implemented in the processing sequence of SiGe solar cells. For this

purpose 2 µm Al were evaporated onto the wafers' rear side followed by a sintering step at 800°C. Furthermore, a Ti/Pd/Ag front grid, defined by an evaporation mask, as well as an Al back contact were evaporated. Finally the samples were annealed in an Ar/H_2 atmosphere and parasitic p-n junctions were separated by dicing resulting in two rectangular solar cells with an area of 2.8 cm^2 each.

5. SOLAR CELL CHARACTERIZATION

IV measurements of the obtained SiGe solar cells resulted in the parameters given in Tab. I. Although both samples have been processed in the same way sample #2 in all respects shows a worse performance than sample #1.

	V_{OC} [mV]	J_{SC} [mA/cm^2]	*FF* [%]	η [%]
SiGe#1	520	13.0	70.8	4.8
SiGe#2	450	11.5	41.6	2.2

Table I: Open Circuit Voltage V_{OC}, short circuit current density J_{SC}, fill factor *FF* and efficiency η of the processed solar cells (no antireflection coating; reflection SiGe#1 >40%, reflection SiGe#2 >35% at 905 nm).

More detailed information can be obtained by considering the dark IV characteristics given in Fig. 6. Except for the voltage range from 0 to 0.5 V both curves are nearly identical. This indicates for equal defect densites in the bulk. However, in the voltage range from 0 to 0.5 V sample #2 shows a much higher dark current density. This is most probably due to shunt like mechanisms within the space charge region which lead to a high saturation current of the second diode defined in the two diode model.

Compared to silicon based cells a higher Internal Quantum Efficiency (IQE) in the long wavelength range is expected for SiGe solar cells. Therefore we have measured the spectral response of the processed cells. The resulting graphs are given in Fig. 7 together with the one of a monocrystalline Cz-silicon based solar cell processed in a similar way using screen printing technique. For each wavelength the IQE of the SiGe solar cells is clearly lower than the corresponding one of the Si cell. On the one hand this is surely due to non optimized processing of the SiGe wafers on the other hand the material quality still has to be enhanced.

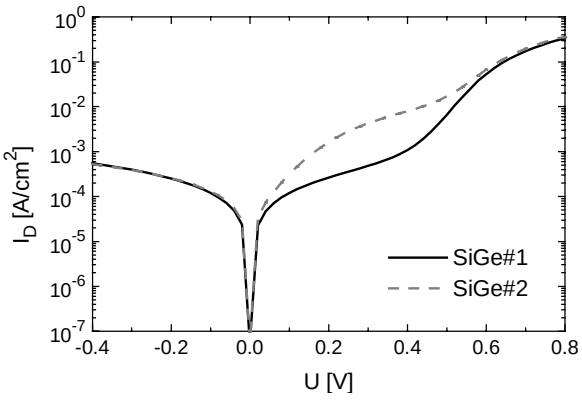

Figure 6: Dark IV characteristics of the SiGe solar cells.

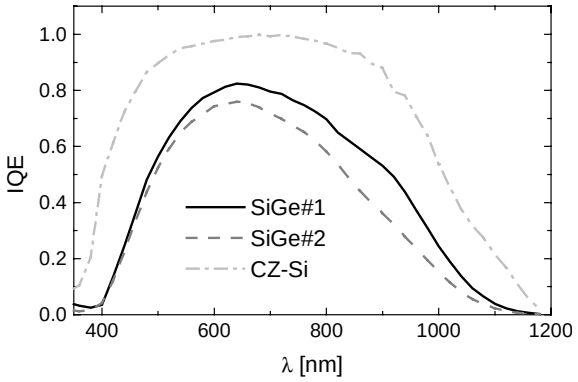

Figure 7: Internal Quantum Efficiencies of processed SiGe solar cells in comparison to a CZ-Si solar cell processed in a similar way.

In order to get more information about the homogeneity of the processed solar cells and the shunt like mechanisms in sample #2 Laser Beam Induced Current (LBIC) mappings have been performed using a laser wavelength of 905 nm and a resolution of 20 µm. In Figs. 8 and 9 the crystal grain structure of the SiGe material can be recognized. This is due to a low IQE of the grain boundaries compared with the efficiency of intragrain regions. In Fig. 8 a quite large variation in performance throughout the cell area is visible. Regions showing a high IQE can be found as well as regions with an insufficiently low quantum efficiency. This leads to the widespread distribution shown in the histogram below the mapping. The worst regions seem to spread in a radial way from a very dark point located at a grain boundary. This indicates for decorated extended crystal defects (e.g. grain boundaries) forming parasitic shunts as mentioned above. Many more of such regions and dark points can be found in Fig. 9. The darkest points can hardly be separated because they lie very close to each other. Consequently they appear as contiguous dark areas now. We hope to get to know more about the reasons for these shunts by future EDX measurements.

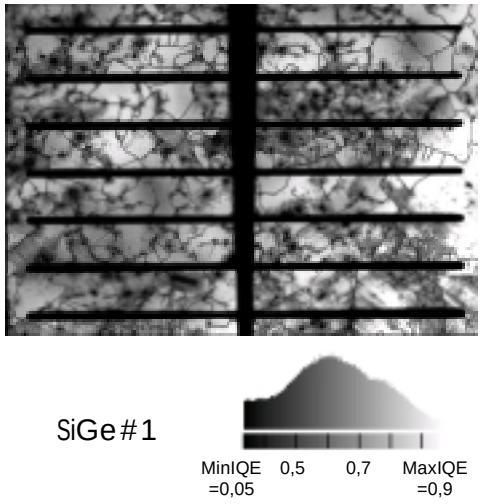

Figure 8: LBIC mapping of solar cell SiGe#1.

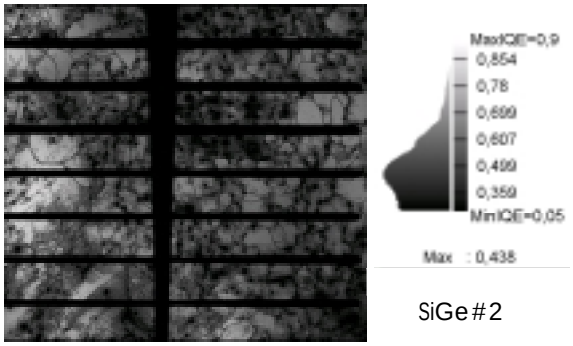

Figure 9: LBIC mapping of solar cell SiGe#2.

CONCLUSIONS

The dominating scattering mechanism in the investigated SiGe samples at room temperature is acoustic phonon scattering as shown by Hall measurements. Fitting the majority charge carrier density results in a slightly lower acceptor activation energy level of boron in SiGe than in Si.

The manufacturing of mc SiGe solar cells based on standard silicon solar cell processing schemes is possible. As shown fill factors above 70% and efficiencies of 4.8% (no ARC) can be reached with non optimized processing steps. However, the IQE in the long wavelength range does not exceed the one of silicon solar cells as predicted by theory. This might be caused by small diffusion lengths, especially as the IQE of the SiGe cells is at every investigated wavelength significantly lower than the one of the monocrystalline Si test wafer. If wafers of enhanced quality and adequate processing parameters were available this behaviour might be different.

At the moment the dominating deleterious effects are low lifetimes and/or regions of parasitic shunts as visible in LBIC mappings. We hope to find out more about the nature of these shunts by future EDX measurements.

ACKNOWLEDGEMENTS

We like to thank J. Hötzel for assistance during screen printing of the solar cells.

REFERENCES

[1] P. Raue, A. Lawerenz, L. Long, M. Rinio, E. Buhrig, H. J. Möller, Proc. 14th European Photovoltaic Solar Energy Conference, Barcelona (1997) 1791.

[2] F. Secco D'Aragona, J. Electrochem. Soc. **119** (1972) 948.

[3] L.J. van der Pauw, A Method of Measuring Specific Resistivity and Hall Effect of Discs of Arbitrary Shape, Philips Res. Repts **13** (1958) 1-9.

[4] K. Seeger, Semiconductor Physics, Springer-Verlag, Wien (1973).

[5] M.A. Green, Solar Cells, Operating Principles, Technology and System Applications, University of New South Wales, Australia (1986).

[6] M. Meuris, P.W. Mertens, A. Opdebeek, H.F. Schmidt, M. Depas, G. Vereecke, M.M. Heyns, A. Philipossian, Solid State Tech. (1995) 109.